

Scattering of 15.7-Mev Electrons by Nuclei*

E. M. LYMAN, A. O. HANSON, AND M. B. SCOTT†
Department of Physics, University of Illinois, Urbana, Illinois
 (Received July 3, 1951)

Electrons removed from the 20-Mev betatron are focused to a 0.08-inch spot about 10 feet from the betatron by a magnetic lens. The electrons impinge on thin foils at the center of a highly evacuated scattering chamber having a diameter of 20 inches. Elastically scattered electrons, selected by a $\frac{3}{8}$ inch \times 2 inch aperture, are focused by means of a 75° magnetic analyzer with 3 percent energy resolution and are detected by coincidence Geiger counters. Corrections are applied for multiple scattering and for energy losses which remove the electrons from the range of energies accepted by the detector arrangement. The scattering cross section for gold at 150° is found to be about 2.6 times that given by Mott's formula in the Born approximation and about one-half of that expected for the scattering by a point nucleus. This result is in good agreement with the calculations for electrons of this energy if the nuclear charge is assumed to be distributed uniformly throughout the nuclear volume.

The results for the scattering from C, Al, Cu, and Ag are also in agreement with the assumption of a uniformly distributed nuclear charge within the uncertainties involved in the theory and the experimental results.

INTRODUCTION

THE scattering of fast electrons by nuclei has been the subject of a large number of researches. The previous work in the energy range above 10 Mev has been done primarily with cloud chambers. The results are quite divergent but could be considered to be in qualitative agreement with theoretical calculations.¹

At lower energies some accurate measurements have been made using electrons accelerated by an electrostatic generator to energies up to 2.25 Mev. These results, reported by Van de Graaff, Buechner, and Feshbach, for several elements and for a number of angles up to 50° are in good agreement with calculations.² The more recent work of Champion and Roy and that of Sigrist³ indicate that the scattering at larger angles is

also in agreement with calculations, although others report divergent results.⁴

It appears that the remaining discrepancies at these energies are due to experimental difficulties, and it will be assumed in this work that the scattering of electrons having energies up to 3 Mev are described by complete calculations^{5,6} based on Mott's formulas for the scattering by a point charge.

At sufficiently high energies, Rose, and more recently Elton, have shown that the scattering of electrons by nuclei would be considerably modified by the fact that the size of the nuclear charge distribution is no longer small compared to the electron wavelength.⁷

An experimental investigation of the scattering of high energy electrons was made feasible by the successful extraction of the electron beam from the 20-Mev betatron. Preliminary results have been reported briefly⁸ and have been compared with the accurate calculations by Elton.⁹

I. APPARATUS AND EXPERIMENTAL METHOD

Production, Extraction, and Focusing of the Electron Beam

The experimental arrangement is shown schematically in Fig. 1. When electrons accelerated in the betatron donut reach 15.7 Mev, as determined by a flux

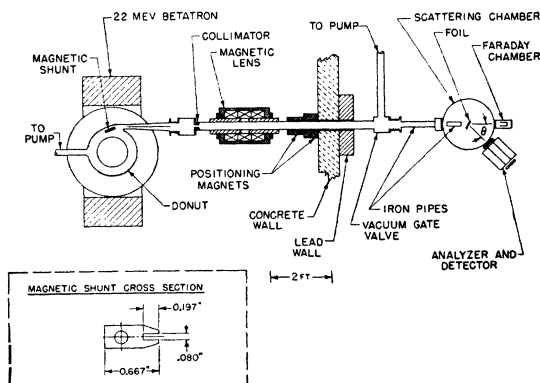


FIG. 1. Schematic showing betatron and scattering chamber.

* Supported by the joint program of ONR and AEC.

† Now at Massachusetts Institute of Technology, Cambridge 39, Massachusetts.

¹ Randels, Chao, and Crane, Phys. Rev. **68**, 64 (1945). See also reference 18, p. 83.

² Van de Graaff, Buechner, and Feshbach, Phys. Rev. **69**, 452 (1946); Buechner, Van de Graaff, Sperduto, Burrill, and Feshbach, Phys. Rev. **72**, 678 (1947).

³ F. C. Champion and R. R. Roy, Proc. Phys. Soc. (London) **61**, 532 (1948); W. Sigrist, Helv. Phys. Acta **16**, 471 (1943).

⁴ Alichanian, Alichanow, and Weissenberg, J. Phys. (USSR) **9**, 280 (1945); W. Bothe, Z. Naturforsch. **4a**, 88 (1949).

Note added in proof:—Paul and Reich have recently reported general agreement with theory at 2.2 Mev except for somewhat low values for gold at 90° and 120°. (Private communication. Work to appear in *Zeitschrift für Physik*.)

⁵ J. H. Bartlett and R. E. Watson, Proc. Am. Acad. Arts Sci. **74**, 53 (1940).

⁶ W. A. McKinley and H. Feshbach, Phys. Rev. **74**, 1759 (1948).

⁷ M. E. Rose, Phys. Rev. **73**, 279 (1948).

⁸ Lyman, Hanson, and Scott, Phys. Rev. **79**, 228 (1950); Phys. Rev. **81**, 309 (1951).

⁹ L. R. B. Elton, Phys. Rev. **79**, 412 (1950); Proc. Phys. Soc. (London) **A63**, 1115 (1950).

integrating circuit,^{10,11} an expansion pulse causes their orbit to spiral outward and enter a magnetic shunt, or field free region,¹² from which they are able to escape the betatron guide field. The shape of the iron laminations comprising the shunt is shown by the inset in Fig. 1. The laminations are separated by mica spacers and the stack, 3.5 in. long, is located tangentially, at a radius of 8.6 in. from the center of the donut. The injector is at a radius of 8.75 in. and the equilibrium orbit is at 7.6 in. The radial position of the magnetic shunt is rather critical; if it is located at too large a radius, the electron beam fails to enter the slot in the shunt; while if it is at too small a radius, the orbit expands into the shunt prematurely before the electrons have reached full energy. The proper orientation of the shunt is accomplished by selsyn remote control while the betatron is in operation.

The spray of electrons emerging from the magnetic shunt is about 1° high and 6° wide. The most intense portion of this beam is selected by a collimator subtending 1° , and passed down the axis of a magnetic lens which focuses it into a spot 0.08 in. in diameter at a point about 10 feet from the betatron. Positioning electromagnets provide a means of fine adjustment of the vertical and horizontal position of the focal spot.

Scattering Chamber, Energy Analyzer, and Detectors

The electron beam enters the scattering chamber shown in Fig. 2 through one of the port holes spaced at intervals of 30° in the cylindrical wall and comes to a focus on the target foil at the center. A thick aluminum faraday chamber diametrically opposite the beam entrance port is connected to a vibrating reed electrometer and serves to measure the charge incident upon the foil. The scattered beam of electrons is selected by a rectangular aperture $\frac{3}{8}$ in. wide and 2 in. high, located in the chamber wall 10 inches from the scattering foil. After passing through the aperture they enter the magnetic analyzer which focuses them upon a group of Geiger counters in coincidence.

The chamber, defining aperture, magnetic analyzer, counters and their shielding are all mounted on a rotating platform with its axis of rotation at the center of the target foil. The angle of scattering is changed by detaching the entrance tube and faraday chamber, rotating the table to the new position, then reconnecting the tube and faraday chamber. During this process, the chamber is isolated from the betatron and diffusion pumps by a system of vacuum gates. While operating, there are no foils or windows anywhere in the path of the incident beam.

Target selection is accomplished remotely by a selsyn system which drives the target holder through 0-ring

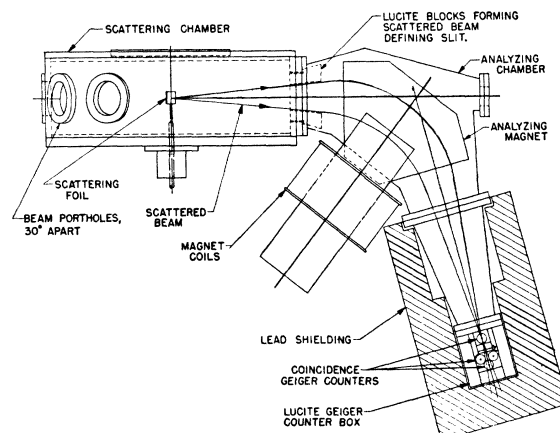


FIG. 2. Scattering chamber.

seals. The target holder has spaces for 10 target foils, a space for a piece of fluorescent x-ray screen used for observation of the beam position and focus, a blank space for transmitting the incident beam directly to the faraday chamber without intervening scattering material, and a 20-mil vertical tungsten wire used for alignment purposes. The scattering angle is read from a vernier scale attached to the stationary part of the framework supporting the rotating platform.

The magnetic analyzer focuses the elastically scattered electrons from the 0.08-inch beam incident on the scattering foils to a line about $\frac{1}{4}$ in. wide and 2 in. long. This beam is more than covered by the Geiger counter which has a diameter of $\frac{3}{4}$ in. and an active length of about 3 inches. The $\frac{3}{4}$ -inch width of the Geiger counter corresponds to an energy range of 3 percent. Hence the maximum count obtained by varying the magnetic field will include all electrons which have lost less than 3 percent of the initial energy.

The field of the analyzer magnet is controlled to 0.1 percent by a servo system which derives its error signal by comparing the voltages developed in two rotating flip coils, one in the magnetic field and the other in a permanent magnet reference field. The position and nature of the focus of the analyzer magnet and its $H\rho$ calibration were determined by the well-known "hot-wire" method using No. 44 copper wire carrying about 1 ampere.

To eliminate serious interaction between the field of the analyzer magnet and the incident beam at large scattering angles, it was found to be necessary to shield the incident beam with iron pipe duct, both outside and inside the chamber.

Experimental Procedure

During the initial stages of extraction of the electron beam and alignment of the apparatus, a telescope, mirrors, and a piece of fluorescent x-ray screen were used to observe the beam position and intensity at various points in its path. First, the orientation of the magnetic shunt was adjusted to produce a small in-

¹⁰ McElhinney, Hanson, Becker, Duffield, and Diven, *Phys. Rev.* **75**, 542 (1949).

¹¹ Katz, McNamara, Forsyth, Halsam, and Johns, *Can. J. Research A28*, 113 (1950).

¹² Skaggs, Almy, Kerst, and Lanzl, *Radiology* **50**, 167 (1948).

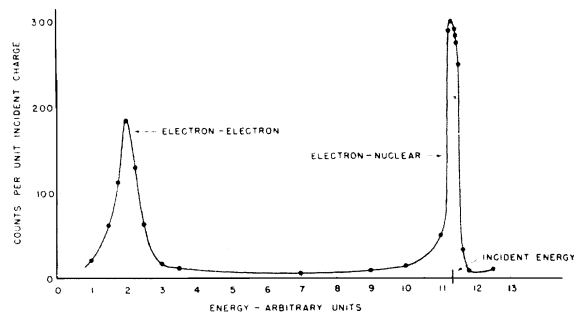


FIG. 3. Energy spectrum of 15.7-Mev electrons scattered at 30° by polystyrene (carbon). The ordinate represents the observed count as a function of the analyzer magnetic field, and does not represent the number of electrons per unit energy interval. The counters have a 3 percent resolution in energy.

tense spot at the exit port of the donut. Next, the duct leading to the scattering chamber was attached, evacuated, and oriented until maximum intensity was obtained at the chamber end. Further fine adjustment was continued with the magnetic lens current turned on, until a small, focused spot was formed centrally at the end of the duct and remained stationary upon reversal of the magnetic lens current, indicating coincidence of source, focal spot and axis of the lens. Under these conditions, the position of the beam was stable for slight variations in energy and magnetic lens current.

The final step in alignment consisted of locating the framework supporting the rotating platform and chamber so that the beam came to focus precisely at the center of the chamber. After careful visual alignment, exact centering was accomplished by placing the 20-mil vertical tungsten wire at the center of the chamber and measuring the beam scattered from it by an auxiliary ionization chamber at 30° . The position of the incident electron beam was then adjusted by the horizontal positioning electromagnet until the scattering was a maximum. It was necessary to repeat the centering adjustment at each scattering angle because of the slight interaction between analyzer field and incident beam.

The vernier dial reading corresponding to zero angle of scattering was determined by adjusting the chamber position until the beam passed centrally through the defining aperture into the detectors. Other scattering angles were read to 0.03° with reference to this position.

The shape and magnitude of the peak due to nuclear scattering and the background were determined for each foil at each angle of scattering. A typical complete spectrum is shown in Fig. 3.

Each point of the spectrum is the number of counts recorded (adjusted for counting-rate losses) while a given charge was being collected by the faraday chamber directly behind the foil. The faraday chamber was connected to a vibrating reed electrometer whose instrumental capacitance was increased by a calibrated polystyrene condenser connected between the input

and inverse feedback terminals. With this connection, the charge was simply the product of voltage change and the capacitance, the effect of all other capacitances being degenerated to insignificance by the feedback.¹³ The charge incident upon the foil was obtained from the charge measured by the faraday chamber and the foil transmission factor. The latter was determined by a series of measurements of the time required to collect a given charge, with the foil present and then absent, at constant beam intensity.

Shielding of the counter system from the x-ray background produced by the betatron was not difficult for scattering at 30° , but at 150° a foot-thick concrete wall and 6 inches of lead surrounding the counters were required.

II. TREATMENT OF DATA

The number of counts corresponding to the maximum of the approximately flat-topped elastic scattering peak for a given incident charge is a measure of the cross section for scattering at any particular angle. The fact that electrons were incident upon the foil in microsecond bursts 180 times per second, made it necessary to correct for the number of counts which correspond to more than one electron passing through the Geiger counters. This correction is given with sufficient accuracy by¹⁴

$$C = C_{\text{obs}}(1 + C_{\text{obs}}/360t), \quad (1)$$

where C_{obs} is the number of counts recorded in t seconds. This correction was applied individually to every observation. In taking the data the counting rate was kept sufficiently low so that this correction did not exceed 10 percent.

A cross section can be obtained from the usual relation

$$\sigma_{\text{obs}} = C/nN\Omega, \quad (2)$$

where C is the count corrected for the above losses minus the count with the scattering foil absent; n is the number of electrons incident on the foil as determined by the charge collected in the faraday chamber and the transmission ratio; N is the number of atoms/cm² in the path of the beam as determined by the weight of the foils and the angle between the normal to the foils and the direction of the incident beam; and Ω is the solid angle determined by the aperture defining the scattered beam.

In comparing experimental cross sections with theory, it was found to be convenient to adjust the observed cross section to take account of (1) the small range of scattering angle of the electrons admitted to the detectors because of the finite size of the defining aperture and the size and angle of convergence of the incident beam, (2) effects due to the finite thickness of the scat-

¹³ Palevsky, Swank, and Grenchick, *Rev. Sci. Instr.* **18**, 298 (1947).

¹⁴ C. H. Westcott, *Proc. Roy. Soc. (London)* **A194**, 508 (1948).

tering foils, and (3) the effect of radiation associated with the single scattering process itself.

In calculating the geometrical corrections, it is sufficient to assume that the angular dependence of the scattering cross section is given by the Mott formula (Born approximation),

$$\sigma_M(\theta) = (Ze^2/2mv^2)^2 (\csc^4 \frac{1}{2}\theta - \beta^2 \csc^2 \frac{1}{2}\theta). \quad (3)$$

It can be shown from spherical trigonometry that an electron which enters the defining aperture making an angle θ_x , θ_y with respect to the line connecting the center of the foil with the center of the aperture has been scattered through an angle

$$\theta = \theta_0 + \theta_x + \frac{1}{2}\theta_y^2 \cot\theta_0, \quad (4)$$

where θ_0 is the scattering angle to the center of the aperture. The average intensity (I_{Av}) over the aperture is then given by

$$I_{Av} = I_0 \left(1 + \frac{\sigma' h^2}{\sigma 24} \cot\theta_0 + \frac{\sigma'' W^2}{\sigma 24} \right), \quad (5)$$

where I_0 is the intensity at θ_0 . W and h represent the angular width and height of the aperture and σ' and σ'' represent derivatives of Eq. (3) with respect to θ . The correction to the observed cross section calculated from this equation resulted in an increase of 1.8 percent at 30° and a decrease of 1.3 percent at 150° , for example. The corrections for the width and angular divergence of the incident beam are negligible when superimposed on the aperture correction.

Multiple scattering of electrons in the foil results in a correction very similar to the aperture correction. Chase and Cox¹⁵ have shown that the combination of single scattering superimposed upon the multiple scattering results in an additional averaging over the multiple scattering distribution such that the average intensity at θ_0 is

$$I = I_0 [1 + \frac{1}{4}\epsilon^2(\sigma' \cot\theta_0 + \sigma'')/\sigma], \quad (6)$$

where ϵ represents the rms value of the multiple scattering distribution (the $1/e$ width, if the distribution is gaussian). In the angular range where the cross section varies as $1/\theta^4$ the above correction agrees with the first order term of the expression given by Butler.¹⁶

At scattering angles exceeding 90° , the scattered electrons must emerge from the same side of the foil as they enter. The probability of a double large angle scattering becomes important because of the increased path length for electrons scattered into the plane of the foil.¹⁷ For example, for scattering at 150° from a foil with its plane perpendicular to the incident beam, the ratio of intensity I to the intensity I_0 due to single scattering alone may be estimated as

$$I/I_0 \approx 1 + [\sigma(90^\circ)\sigma(60^\circ)N\pi/\sigma(150^\circ)]. \quad (7)$$

¹⁵ C. T. Chase and R. T. Cox, Phys. Rev. **58**, 246 (1940).

¹⁶ S. T. Butler, Proc. Phys. Soc. (London) **A63**, 599 (1950).

¹⁷ G. Goertzel and R. T. Cox, Phys. Rev. **63**, 37 (1943).

Since the correction is proportional to the thickness of the foil, it may be determined experimentally by comparing the scattering from thick and thin foils of the same element. For the thin Au foil, the experimentally determined correction was 1.8 ± 1.0 percent while that determined from Eq. (7) was 0.3 percent. The discrepancy between the experimental and calculated correction is in qualitative agreement with that observed by Shull, Chase, and Myers.¹⁸

The correction for loss of electrons from the peak due to energy degradation in electron-electron collisions is found by determining the fraction that lose more than 3 percent of their energy in traversing the foil. The effective cross section for loss of energy between E and $E+dE$ in a single small angle electron-electron collision is¹⁹

$$pdE \simeq (2\pi e^4/mv^2)(dE/E^2). \quad (8)$$

The cross section for the loss of more than 3 percent of the energy of a 15.7-Mev electron obtained by integrating Eq. (8) is found to be 0.542 barn per electron in the foil.

In addition to the correction for energy losses due to single electron-electron collisions, a small correction is included to account for the effect of double collisions in which the energy loss per collision is less than 3 percent.

The correction for loss of electrons from the peak due to energy degradation by radiation in small-angle nuclear collisions is found by calculating the number of photons produced whose energies exceed $0.03E_0$. For 15.7-Mev electrons, the number of such photons produced per Mev radiation loss by an electron is found from the bremsstrahlung spectrum to be 0.291 photon, where the total radiation loss is given by Heitler.²⁰ The fraction of electrons which lose 3 percent or more of their energy, and will therefore escape detection is approximately equal to 0.291 times the total radiation loss in the foil.

Superimposed on the energy losses of electrons in penetrating a foil, which are in all cases proportional to the thickness of the foil, is another radiative loss associated with the single large angle scattering being observed. This energy loss has a distribution qualitatively similar to the average bremsstrahlung spectrum radiated by electrons. There will therefore be no electrons which are scattered strictly elastically. Most will be scattered with small radiative losses and a certain number will fall out of the energy range ΔE accepted by the counters. This correction can be obtained from a calculation by Schwinger²¹ which includes the reduction in cross section associated with the energy

¹⁸ Shull, Chase, and Myers, Phys. Rev. **63**, 29 (1943).

¹⁹ Mott and Massey, *Theory of Atomic Collisions* (Oxford University Press, London, 1949), second edition, p. 369.

²⁰ Heitler, *Quantum Theory of Radiation* (Oxford University Press, London, 1945), second edition, p. 191.

²¹ J. Schwinger, Phys. Rev. **76**, 790 (1949); see also reference 19, p. 379.

TABLE I. Typical corrections. Percent corrections added to observed cross sections for thin and thick gold foils.

	30°		60°		90°		120°		150°	
	Thin	Thick	Thin	Thick	Thin	Thick	Thin	Thick	Thin	Thick
Multiple scattering	-1.0	-5.9	-0.3	-1.8	-0.2	-1.3	-0.2	-1.0	-0.3	-1.8
Radiation straggling	0.4	1.7	0.4	1.9	0.5	2.3	0.4	1.9	0.4	1.7
Electron-electron straggling	0.1	0.3	0.1	0.4	0.1	0.5	0.1	0.4	0.1	0.3
Double scattering	0	0	0	0	0	0	-0.5	-2.9	-1.7	-10.1
Schwinger formula (9)	5.4	5.4	7.0	7.0	7.9	7.9	8.5	8.5	9.1	9.1
Aperture size	1.8	1.8	0.3	0.3	-0.1	-0.1	-0.3	-0.3	-1.3	-1.3

loss ΔE as well as the effect of the more complete treatment of the interaction of the electron with the radiation field. This reduction in the cross section is given by the equation

$$\delta = \frac{4}{137\pi} \left[\left(\ln \frac{E}{\Delta E} - \frac{13}{12} \right) \left(\ln \left[\frac{2p_0 \sin \frac{1}{2}\theta}{K} \right] - \frac{1}{2} \right) + \frac{17}{72} + \frac{1}{2} \sin^2 \frac{1}{2}\theta F(\theta) \right], \quad (9)$$

where, for this work, $F(\theta)$ may be taken as unity, $\Delta E/E=0.03$, and $p_0/K=31.7$. The large part of this correction can be seen to be associated with the radiative losses. In order to put the observed results in a form which is independent of the energy band ΔE , accepted by the detectors the observed cross sections have been increased by the factor $1/(1-\delta)$. Values of δ for various angles are given in Table I. These values are taken as the same for all materials, although the calculation is not expected to be accurate for high Z materials.

The magnitudes of the corrections applied to the observed scattering cross sections for a typical element at various angles are summarized in Table I. This table is also representative of the other foils, since they were chosen to have approximately the same NZ^2 . It can be seen that the effect of multiple scattering and energy straggling is small, especially for the thin foil. The corrections for the radiation loss associated with large angle scattering (δ) and the aperture correction are independent of the scattering material. The effect of double scattering is appreciable only at 120° and 150°. As mentioned previously, the magnitude of this correction was estimated from the variation of the observed scattering from two foils of the same material having different thicknesses, and is rather uncertain. Since these corrections are considerably larger than those calculated for this effect the increased scattering attributed here to double scattering may in part have some other interpretation.

It should be pointed out that the data from the thicker foils were not considered as reliable as those from the thinner foils and were used primarily to check or to determine the corrections which were applied to the thin target data.

III. EXPERIMENTAL RESULTS

The scattering cross sections measured for C, Al, Cu, Ag, and Au at scattering angles ranging from 30° to 150° are given in Table II. The numbers of atoms/cm² of the scattering foils are listed in column 2. In column 3, row a, are the observed, unadjusted scattering cross sections at 30° in barns per unit solid angle while in column 3, row b, are the same cross sections corrected for the effects listed in Table I, except for the correction calculated from the Schwinger formula. (This correction is not a function of foil thickness.) In column 4, the estimated standard error is given for the cases of the thin foils. Similar data for the other angles are given in columns 5 to 12.

The results listed in Table II were obtained from the last of a series of 5 runs, taken over a period of a year, during which a great effort was made to decrease random errors and eliminate all sources of systematic error.

The estimated standard errors shown in Table II are based solely upon the sources of random error in the experiment. For the majority of the points, the error due to counting statistics is about 1.2 percent, but at 150° due to low count and large background, it is about 3 percent on the average. In the case of polystyrene, which gave the lowest ratio of counts to background, the error is 10 percent. The estimated error in reading the meter which measured the charge incident upon the foil is 1 percent, in determining the foil transmission factor, 1 percent, and in measurement of the scattering angle (because of the uncertainty in locating the exact position of the incident beam), 1 percent. The total random errors for most of the points are then estimated to be of the order of 2 percent.

The number of atoms/cm² in the foils was determined by weighing an accurately cut area of the foil. Most foils were uniform to within 1 percent. The thinnest gold foil (10⁻⁴ inch) exhibited a thickness variation of 2 percent over the region struck by the incident beam.

The solid angle of the scattered beam admitted to the detector was the same for all angles and any error in it would affect all data equally. Two types of material for defining the aperture were tried; Lucite, 3 inches thick with sides curved to match the electron trajectories and gold, $\frac{1}{16}$ inch thick, backed by lead. The scattering cross sections observed with the two types of apertures were identical to within 1 percent.

TABLE II. Observed and adjusted scattering cross sections.

Element	$N/\text{cm}^2 \times 10^{20}$	30°		60°		90°		120°		150°	
		σ	%	$\sigma \times 10^{+1}$	%	$\sigma \times 10^{+2}$	%	$\sigma \times 10^{+3}$	%	$\sigma \times 10^{+4}$	%
C	11.18 ^a	0.1501		0.08305		0.1230		0.2881		0.4500	
Polystyrene	^b	0.1502	2.4	0.08340	2.0	0.1238	2.4	0.2887	3.4	0.4476	10
Al	3.050 ^a	0.7078		0.3940		0.6447		
	15.21 ^a	0.7126		0.3881		0.6571		1.455		2.652	
	3.050 ^b	0.7065	2.2	0.3951	2.0	0.6477	1.8	
	15.21 ^b	0.7017		0.3932		0.6713		1.455	2.1	2.510	4.5
Cu	2.339 ^a	3.663		2.271		3.860		8.680		14.00	
	6.895 ^a	3.785		2.311		3.737		8.685		15.68	
	2.339 ^b	3.615	2.2	2.283	1.9	3.899	1.8	8.651	2	13.48	3.9
	6.895 ^b	3.596		2.339		3.835		8.529		13.57	
Ag	0.3889 ^a	10.82		7.045		12.31		28.28		...	
	1.143 ^a	10.93		7.105		12.67		28.60		51.30	
	0.3889 ^b	10.78	2.3	7.057	2	12.36	1.8	28.27	2.2	...	
	1.143 ^b	10.74		7.165		12.79		28.43		48.83	3.2
Au	0.1726 ^a	33.67		25.30		49.65		134.2		323.5	
	0.7814 ^a	35.63		28.71		51.11		124.3		247.9	
	0.1726 ^b	33.49	2.2	25.36	2.0	49.87	2.1	133.9	2	228.8	3.8
	0.7814 ^b	34.25		28.84		51.87		122.2		223.5	

^a Observed.^b Corrected for geometry, multiple scattering, $e-e$ collisions, double scattering at large angles, and radiation in small-angle collisions.

Other tests indicated that the counting rates were proportional to the area of the aperture.

The ability of the thick-walled aluminum faraday chamber to retain all of the electron charge collected by it was tested by placing a lead disk at the bottom of the chamber to increase the scattering and the number of x-rays produced by the incident beam. It was found that the total charge retained by the chamber was 3 percent less with the lead bottom than with the usual all-aluminum chamber. From this it was estimated that the loss of charge by the standard aluminum chamber was about 1 percent.

IV. THEORY

In order to discuss the observed results it is convenient to display the ratio of the observed scattering cross sections to that calculated from the simple Mott formula. This formula has already been given as Eq. (3) and accounts for the very large variations in the cross sections. It is expected to represent the observed scattering at small angles for all values of Z and the scattering at all angles for very low Z .

McKinley and Feshbach⁶ have given another formula which is essentially a first-order correction to the simple Mott formula. By their relation the ratio of the coulomb scattering to that given by Eq. (3) is

$$\frac{\sigma}{\sigma_M} = 1 + \frac{\pi Z \beta \sin \theta / 2 [1 - \sin(\theta/2)]}{137 [1 - \beta^2 \sin^2(\theta/2)]} \quad (10)$$

McKinley and Feshbach also obtained an expression involving terms to the fourth power of α , where $\alpha = Z/137$. These results, which will be referred to as the α^4 approximation, should be reliable for higher values of

Z but are not good for the heavy elements where α is not small compared to unity.

The accurate evaluation of Mott's theory for the scattering of electrons by a heavy element is a difficult task and has been carried out in detail for ($Z=80$) by Bartlett and Watson using numerical methods,⁵ and only recently for $Z=47$.²²

The calculated values of σ_M and σ_c/σ_M for 15.7-Mev electrons are given in Table III. The values of σ_c/σ_M for carbon were calculated from Eq. (10). The values for copper are based on the α^4 approximation for $\beta=1$ as calculated by Acheson.²³ The values for silver are those given by Feshbach²² and those for gold are obtained by a small extrapolation of the results of Bartlett and Watson to $Z=79$ and to $\beta=1$.²⁴

A rough experimental check on the reliability of the calculations was made by reducing the energy of the electrons to 4.6 Mev during one of the runs at 150 degrees. Although the multiple and double scattering corrections were large the relative values were still fairly good for those foils where the corrections were about the same. The ratio of the scattering from gold and silver to that from aluminum was found to be in good agreement with the calculated ratio. The accuracy of these relative measurements was not high but the results lend support to the conclusion that the scatter-

²² Private communication from H. Feshbach giving F and G values for high energy electrons on silver.

²³ L. K. Acheson Jr., Phys. Rev. **82**, 488 (1951). We are indebted to Professor Feshbach for informing us of these calculations before publication.

²⁴ We are indebted to Professor Bartlett for assistance in extrapolating the calculations so as to be applicable to gold at these energies.

TABLE III. Calculated values for scattering from a point charge. (σ_M in barns per steradian).

Z	$\beta^2 = 0.999$				$E = 31.72 \text{ mc}^2$		Kinetic energy = 15.7 Mev			
	30°		60°		90°		120°		150°	
	σ_M	σ_c/σ_M	$\sigma_M \times 10^2$	σ_c/σ_M	$\sigma_M \times 10^2$	σ_c/σ_M	$\sigma_M \times 10^4$	σ_c/σ_M	$\sigma_M \times 10^4$	σ_c/σ_M
6	0.1481	1.029	0.855	1.045	0.1425	1.057	3.17	1.063	0.566	1.067
13	0.6950	1.069	4.01	1.112	0.6692	1.143	14.9	1.154	2.608	1.154
29	3.459	1.165	19.97	1.300	3.330	1.387	74.1	1.444	12.98	1.437
47	9.085	1.300	52.44	1.630	8.747	1.852	194.6	2.126	34.09	2.211
79	25.67	1.456	148.2	2.482	24.71	3.795	550	4.828	96.3	5.54

ing theory, when completely evaluated, is sufficient to describe the observed results at lower energies.

Since the wavelength for 15.7-Mev electrons is comparable with nuclear dimensions, the observed scattering is reduced somewhat from that expected for the scattering by a point charge.

For light nuclei where the Born approximation expresses the scattering with reasonable accuracy, the ratio of scattering from a uniform charge distribution of radius R to that from a point charge can be expressed by the relation,^{7,9}

$$\sigma/\sigma_c = [(3/K^3 R^3)(\sin KR - KR \cos KR)]^2 \quad (11)$$

where K is the change in wave number associated with the angle of scattering as expressed by the relation $K = (2p/\hbar)\sin\frac{1}{2}\theta = (1.64 \times 10^{12} \sin\frac{1}{2}\theta \text{ cm}^{-1})$. Although this relation is not accurate for any but the lightest nuclei, it is useful in estimating the magnitude of the effect and the manner in which the cross section depends on the nuclear radius.

Elton and Acheson have treated the size effect in more detail and have derived expressions for the reduction in the cross sections which should be quite reliable. In particular, Acheson²³ has shown that the effect of the finite distribution of the nuclear charge can be expressed in terms of the change in a single phase shift δ_1 in what corresponds to the S wave. According to Acheson the ratio can be written

$$\frac{\sigma}{\sigma_c} = 1 + \frac{4 \cos^2 \frac{1}{2} \theta}{|G|^2} \text{Re} \left[G e^{-2i\chi_1} \left(\frac{e^{2i\delta_1} - 1}{2i} \right)^* \right] + \frac{4 \cos^4 \frac{1}{2} \theta}{|G|^2} \sin^2 \delta_1, \quad (12)$$

TABLE IV. Theoretical and experimental ratios of the scattering to that from a point charge. (σ/σ_c).

	U	30°		60°		90°		120°		150°	
		S	U	S	U	S	U	S	U	S	
C Theory	0.996	0.993	0.984	0.976	0.972	0.952	0.956	0.928	0.927	0.910	
Al Theory	0.992	1.003	0.971	1.004	0.948	0.942	0.878	0.897	0.915	0.833	
Cu Theory	0.981	1.006	0.928	0.952	0.880	0.872	0.920	0.925	0.864	0.823	
Ag Theory	0.962	0.948	0.863	0.945	0.880	0.754	0.916	0.760	0.794	0.574	
Au Theory	0.991	0.966	0.77	0.887	0.656	0.685	0.916	0.656	0.685	0.512	
exp't	0.978	0.973	0.741	0.672	0.57	0.828	0.425	0.45	0.747	0.262	
								0.551	0.292	0.472	

²³ Cook, McMillan, Petersen, and Sewell, Phys. Rev. **75**, 7 (1949); J. DeJuren and N. Knable, Phys. Rev. **77**, 606 (1950); H. Lu, Phys. Rev. **77**, 416 (1950).

where G is the complex function determining the coulomb scattering in the approximation that $\beta = 1$, χ_1 is the first-order phase shift for the scattering by a coulomb field, and $\delta_1 = \eta_1 - \chi_1$ is the change in the phase shift for the given charge distribution.

It may be pointed out that the ratio σ/σ_c is not independent of σ_c since $\sigma_c = \lambda^2 |G|^2 \sec^2 \frac{1}{2} \theta$. Therefore, a calculation which gives too small a value for σ_c will at the same time predict too large a decrease in the ratio σ/σ_c for any given charge distribution. The experimental values for σ/σ_c for a given element as a function of angle are sufficient to determine only one constant, namely, δ_1 . It is, therefore, not possible to use these results to determine the nuclear radius as well as the charge distribution.

Since there are several methods of measuring nuclear radii the values of the phase shifts determined from the present experiments may be used to distinguish between various possible nuclear charge distributions. For a given nuclear radius the phase shift for the case where the nuclear charge is distributed over the surface of the nuclear volume will be about 50 percent larger than that for the charge distributed uniformly throughout the nuclear volume. The deviations from coulomb scattering [Eq. (12)] will also be different by about 50 percent for these two cases. The difference for the heaviest elements is large enough to be experimentally distinguishable at this energy.

Recent determinations of nuclear radii as obtained from the scattering of fast neutrons indicate that on the average the radii are given by the relation $R = 1.37 A^{1/3} \times 10^{-13}$.²⁵ This radius does not include the range of nuclear forces and should represent the effective radius

containing all nuclear particles. It does not necessarily follow that the nuclear protons are distributed over this entire volume but this is the simplest assumption.

The values for σ/σ_c as based on the work of Acheson are given in Table IV for cases of uniform and surface distributions.

V. DISCUSSION OF RESULTS

Before comparing the experimental results with the calculations of the previous section it is necessary to make the adjustment discussed previously for the effect of radiative losses associated with the observed scattering. The experimental arrangement used was not designed to check this effect accurately and hence there is only indirect experimental evidence that the correction as calculated by Schwinger and shown in Table I is correct. The agreement of the results with theory, however, is better when the radiative correction is applied. This is particularly true in the case of polystyrene and aluminum scatterers. A systematic error, such as an error in the energy of the incident beam or an error in measuring the charge incident on the foil, which could change all the observed cross sections uniformly might be wrongly interpreted in terms of a larger or smaller radiative correction. The tabulated values of δ are not expected to be accurate for high values of Z , but are used here since there are no better calculations available.

The experimental cross sections, therefore, have been adjusted for the radiative losses, δ , and are presented as ratios to the point charge scattering in Table IV. The adjusted data are shown in Fig. 4 as ratios to the simple Mott formula. This plot shows very clearly the way the scattering deviates from the simple formula. The adjusted data are presented as ratios to coulomb scattering in Fig. 5. The solid lines in this figure represent the theoretical values for a uniform nuclear charge distribution over a radius given by $1.45A^{1/3} \times 10^{-13}$ cm as used by Acheson.

Upon comparing the experimental results with the calculated values the following conclusions might be drawn. In the case of gold where the decrease in the scattering is the greatest, the results agree fairly well with the assumption that the charge is distributed uniformly over the usually accepted nuclear volume. It is apparent that the agreement would be somewhat better if a radius about 20 percent smaller than that shown in the figure is used. This indicates that the proton distribution might be more densely packed toward the center of the nucleus as suggested by Born and Yang.²⁶

If it is assumed that the charge density is distributed uniformly over the surface of the nuclear volume, it is found that the observed phase shift would give a nuclear radius for gold almost a factor of two smaller than that usually accepted. Although there are reasons to expect a charge distribution which has the greatest density toward the outside of the nucleus, the present

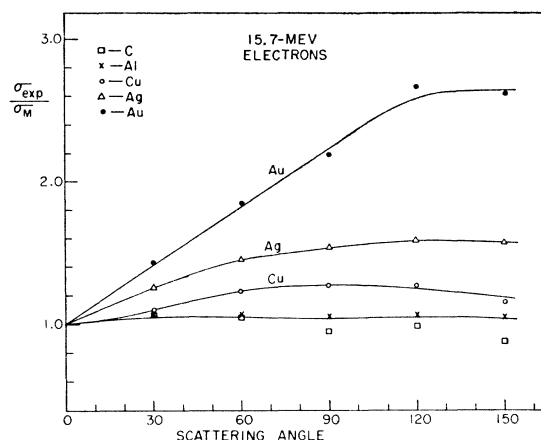


FIG. 4. Experimental results after correcting for counting losses due to radiation. The results are shown here as ratios to the simple Mott formula, Eq. (3). The solid lines sketched in are used merely to connect the experimental data and have no theoretical significance.

measurements seem to exclude this distribution. The decrease in the cross section for silver can also be explained in terms of a uniform distribution of charge over a 20 percent smaller radius.

It is difficult to say much about nuclear size in the cases of C, Al, and Cu since the reduction from coulomb scattering is small and of the same order of magnitude as the uncertainties in the measurements. The over-all

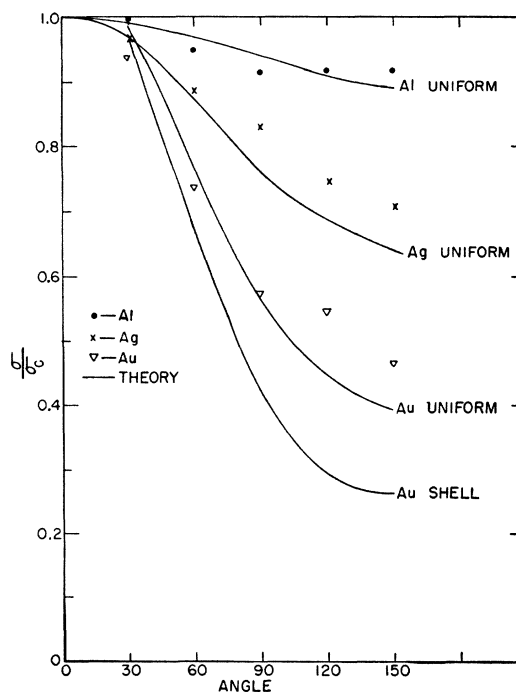


FIG. 5. Experimental results, as in Fig. 4, shown as ratios to coulomb scattering. The solid lines represent the calculated reduction in scattering for nuclear radii given by $R = 1.45A^{1/3} \times 10^{-13}$. Calculated curves are shown only for a uniform distribution of charge except for gold where the curve for a surface charge distribution is also shown.

²⁶ M. Born and L. M. Yang, *Nature* **166**, 399 (1950).

data, however, agree better with the calculations for a uniform charge distribution than for the surface charge distribution.

VI. SUMMARY

The observed scattering of 15.7-Mev electrons by nuclei is compared with the calculations of Elton and of Acheson on the assumption that the radiation correction as calculated by Schwinger is valid. The observed deviations from coulomb scattering are consistent with the picture of a nuclear charge whose radius is given by the neutron experiments and whose density distribution is uniform or possibly slightly greater at the center of the nucleus.

We wish to express our appreciation to S. M. Dancoff and S. Drell for preliminary discussions, to M. E. Rose and L. R. B. Elton for communications regarding the earlier results, and to J. H. Bartlett and J. M. Blatt for discussions regarding the calculations and the interpretation of the results. We are particularly indebted to H. Feshbach for his kind cooperation in sending us the results of pertinent calculations in advance of publication.

The valuable assistance of D. E. Riesen, J. R. Leiss, A. J. Petersen, A. R. Olson, F. Schroeder, K. Hiroshige, and B. A. Smith in building some of the equipment and carrying out the measurements is gratefully acknowledged.

Measurement of Multiple Scattering of 15.7-Mev Electrons*

A. O. HANSON, L. H. LANZL,[†] E. M. LYMAN, AND M. B. SCOTT[‡]
Department of Physics, University of Illinois, Urbana, Illinois

(Received July 3, 1951)

The angular distribution of electrons scattered by thin Be and Au foils has been measured for angles where the multiple scattering is important. The $1/e$ widths of the distributions obtained with Au foils of 18.66 and 37.28 mg/cm² are 2.58° and 3.76°, respectively. These widths are about 10 percent narrower than those calculated from the theories of Williams or of Goudsmit and Saunderson but are in good agreement with the calculations of Molière.

The $1/e$ widths obtained with Be foils of 257 and 495 mg/cm² are 3.06° and 4.25°. These widths are about 5 percent smaller than those given by Molière's theory increased by $(1+1/Z)^{1/2}$ for

the contribution of electron-electron collisions. The discrepancy may be qualitatively explained by the fact that the Thomas-Fermi screening used in the calculation is different from the effective screening in the Be metal.

The scattering from the two Au foils was measured for larger angles where the scattering can be considered as single scattering modified by the effect of multiple scattering. The ratio of the scattering from the thick to the thin foil can be represented by the relation $2+95/\theta^2$ from 9° to 30°, and is in fair agreement with theoretical expressions for this ratio.

THERE have been a number of experimental investigations of the scattering of electrons by multiple collisions in passing through various materials. The most complete series of experiments has been carried out by Kulchitsky *et al.*,¹ who investigated the scattering of 2.25-Mev electrons by elements from lithium to lead. They found that their results were in agreement with the theories of Williams² and of Goudsmit and Saunderson³ for the light elements if the electron-electron scattering were accounted for by increasing the width calculated for nuclear collisions by a factor $(1+1/Z)^{1/2}$. Their results for the heavy nuclei, however, gave widths which were from 10 to 15 percent narrower than predicted by the theories mentioned.

The present work⁴ with higher energy electrons confirms the above results. It will be shown that the experimental results to be presented here, as well as those of Kulchitsky *et al.*, are in better agreement with the theory of Molière,⁵ who has investigated the basic single scattering law at small angles, which enters into the theory, in more detail than other authors.

A brief resumé of the various theories is given by Groetzinger, Berger, and Ribe,⁶ in connection with the discussion of some cloud chamber observations.

EXPERIMENTAL METHOD

The experimental arrangement used was the same as that described in the work on electron-electron scattering⁷ except for the insertion of a smaller aperture defining the scattered beam, and the use of a different detector.

* Supported by the joint program of the ONR and AEC.

[†] Now at Argonne National Laboratory, Chicago, Illinois.

[‡] Now at Massachusetts Institute of Technology, Cambridge 39, Massachusetts.

¹ L. A. Kulchitsky and G. D. Latyshev, *Phys. Rev.* **61**, 254 (1942); Andrievsky, Kulchitsky, and Latyshev, *J. Phys. USSR* **6**, 279 (1943).

² E. J. Williams, *Phys. Rev.* **58**, 306 (1940).

³ S. Goudsmit and J. L. Saunderson, *Phys. Rev.* **58**, 36 (1940).

⁴ Preliminary results were reported at the Chicago meeting of the Physical Society, *Phys. Rev.* **81**, 309 (1951).

⁵ G. Molière, *Z. Naturforsch.* **3a**, 78 (1948); **2a**, 133 (1947).

⁶ Groetzinger, Berger, and Ribe, *Phys. Rev.* **77**, 584 (1950). See also Mott and Massey, *The Theory of Atomic Collisions* (Oxford University Press, London, 1949), second edition, p. 193.

⁷ Scott, Hanson, and Lyman, *Phys. Rev.* **84**, 638 (1951).